Comprehensive antibody profiling of mRNA vaccination in children

Authors: Yannic C Bartsch[1], Kerri J St Denis[1], Paulina Kaplonek[1], Jaewon Kang[1], Evan C. Lam[1], Eva J Farkas[2], Jameson Davis[2], Brittany Boribong[2], Wayne Shreffler[3], Alejandro B Balazs[1], Lael M Yonker[2*], Galit Alter[1*]

Affiliations:
[1] Ragon Institute of MGH, MIT, and Harvard; Cambridge, MA, USA
[2] Massachusetts General Hospital, Mucosal Immunology and Biology Research Center; Boston, MA, USA
[3] Food Allergy Center, Massachusetts General Hospital, Division of Pediatric Allergy and Immunology; Boston, Massachusetts

*correspondence: LYONKER@mgh.harvard.edu and GALTER@mgh.harvard.edu

Abstract: With the emergence of SARS-CoV-2 variants, fluctuating mask mandates, and school re-openings, increased infections and disease surged among children recently. Thus, there is an urgent need for COVID-19 vaccines for children of all ages. However, whether young children will respond appropriately to mRNA vaccines remains unclear. Here, we deeply profiled the vaccine-induced humoral immune response in 7-11 year old children receiving the mRNA-1273 vaccine. Vaccinated children induced significantly higher antibody titers and functions compared to naturally infected children. Moreover, we observed comparable SARS-CoV-2 titers and neutralizing activity across variants of concern and superior Fcγ-receptor binding and phagocytic antibodies in children compared to vaccinated adults. Our data indicate that mRNA vaccination elicits robust antibody responses and drives superior antibody functionality in children.

One-Sentence Summary: mRNA vaccination elicits robust humoral immune responses to SARS-CoV-2 in children 7-11 years of age.

Main Text:

The speed and quality of vaccine development experienced during the COVID-19 pandemic have clearly changed vaccine development for the future. The new platforms responded rapidly to the novel threat, demonstrating robust levels of efficacy (*1, 2*). However, despite the successes of the vaccines, the global roll out has begun to highlight key vulnerable populations, and strategic gaps, that may limit the impact of vaccination globally. Children represent a key vulnerable population, that have been, for the most part, relatively spared from severe disease over the COVID-19 pandemic, but harbor robust, high levels of viral replication and contribute significantly to viral spread (*3-6*). However, in the wake of fluctuating mask mandates, school re-openings, and the rapid spread of the highly infectious SARS-CoV-2 delta variant, a surge of SARS-CoV-2 infections in children has been observed (*7, 8*). Because of the increasing incidence of severe cases in children, the unpredictable development of delayed, life-threatening Multisystem Inflammatory Syndrome in Children (MIS-C), and our evolving awareness of children in the spread of the pandemic, there is an urgent need to roll out vaccines across all ages. However, because children harbor a more naïve immune system that evolves with age, it was uncertain whether the novel vaccine platforms would be sufficiently immunogenic in young children (*9*). Here we deeply characterized the immune response induced in children (n=12; median age= 9 years range: 7 – 11 years; 42% female) that received two doses of the 100μg mRNA-1273 (Moderna) vaccine at days 0 and 28, matching the recommendations and EUA approved dose and scheduling recommendations for adults. This matched dosing enabled the direct comparison of immune profiles across children and adults. Plasma samples were collected before vaccination (V0), approximately four weeks after prime (V1) and four weeks after boost (V2) immunization.

To begin to investigate the vaccine-induced humoral responses we profiled SARS-CoV-2 Spike (S) specific antibody titers. mRNA vaccination in children induced Spike-specific IgM, IgA and IgG1 binding titers following the primary vaccination (V1) with mRNA-1273 (**Figure 1A-B**). Both S-specific IgA1 and IgG1 boosted with the second dose, while S-specific IgM responses declined slightly, marking efficient class switching. Compared to fully vaccinated adults (n=14), children had significantly reduced SARS-CoV-2 S specific IgM and IgA1 levels after second dose but generated slightly higher IgG1 binding titers (**Figure 1C**). Furthermore, vaccine-induced IgG1 titers at both timepoints exceeded titers observed in acute pediatric COVID-19 (n=8) and Multi-Inflammatory Syndrome in Children (MIS-C) (n=6) (**Figure 1A**). All children generated

neutralizing antibodies after the primary immunization (V1) that further expanded after the secondary dose (V2) in all children, resulting in levels comparable, if not slightly higher than observed in adults (**Figure 1B-C**). Again, neutralizing antibody levels in mRNA immunized children were higher than those detected in children with acute COVID-19 or MIS-C. These data are in line with large epidemiologic studies demonstrating an age-dependent shift towards more IgA selection with age as well as the observation of higher IgA titers in COVID-19 infected adults, irrespective of disease severity, compared to children (*10*, *11*). Thus, these data from natural infection and vaccination point to an age-dependent differential selection of antibody isotypes, where children may rely more heavily on IgG, whereas adults may rely on all isotypes. While this profile may be beneficial for SARS-CoV-2 viral control, it is plausible that this bias in isotype selection may render children more vulnerable to other mucosal infections, such as influenza or respiratory syncytial virus (RSV). Thus, future efforts in pediatric vaccine development may require novel strategies, distinct from those used in adults, to selectively improve IgA immunity, via adjuvants or alternate vaccine routes, to promote more effective immunity in children.

In addition to binding and neutralization, protection against severe adult COVID-19 has been linked to additional antibody effector functions, including opsonophagocytic and cytotoxic functions of antibodies(*12-14*). Thus, we profiled the ability of vaccine-induced immune responses to bind to Fc-receptors (FcγR2a, FcγR2b, FcγR3a, FcγR3b, and FcαR) and elicit antibody-dependent complement deposition (ADCD), antibody-dependent neutrophil phagocytosis (ADNP), antibody-dependent monocyte phagocytosis (ADCP), or activation antibody dependent NK cell activation (ADNKA). Children elicited S-specific IgG antibodies that bound robustly to all Fc-receptors following the first dose (**Figure 2A**), markedly greater than responses seen in natural COVID-19 infection or MIS-C. Moreover, these responses expanded further after the second immunization. Interestingly, this increased Fc-receptor binding was not linked to changes in Spike-specific IgG subclass selection (**Supplemental Figure 1**). In contrast, children when compared to adults, induced lower levels of IgA antibodies that were able to interact with the IgA-Fc-receptor, FcαR, in line with the lower levels of IgA generated in children after vaccination as well as after infection (**Figure 2B and Supplemental Figure 2**)(*11, 15*).

To next determine whether these elevated FcγR binding profiles in children translated to more functional Spike-specific immune responses in children, we examined vaccine-induced Fc-effector functions (**Figure 2C**). Interestingly, variable antibody effector functions were observed in

children after vaccination. Low levels of ADCD and ADNP were induced after the primary immunization, followed by a more significant increase in complement depositing and neutrophil phagocytic functions after the boost, resulting in comparable levels of ADCD and increased ANDP in children compared to adults (**Figure 2C-D**). Conversely, a more significant increase in monocyte phagocytosis (ADCP) was observed in children after the prime, that ultimately reached significantly higher levels than adults after the second immunization. Interestingly, opsonophagocytic functions of antibodies, rather than neutralization alone, have been linked to survival of COVID-19 following natural infection (*12*) and are associated with protection from infection in animal models (*16, 17*). In contrast, while NK cell functions (as measured by MIP-1b expression) were induced in only a subset of adults, NK cell activating functions were lower following mRNA vaccination in the children. Furthermore, no difference was noted in antibody binding responses across different Spike domains, pointing to limited differences in antibody targeting across the groups (**Figure 2E**), suggesting that alternate mechanisms likely account for augmented humoral immune function in children, potentially via altered antibody Fc-glycosylation (*18*). Overall, children induced higher levels of ADNP and ADCP recruiting antibodies compared to adults following the full vaccine regimen (**Figure 2D**), whereas adults harbored marginally higher NK cell activating antibodies, pointing to overall functional variation in vaccine quality in children.

To begin to define whether any significant vulnerabilities exist in the humoral immune response in children, we next utilized a machine learning approach to identify the Spike-specific humoral immune features that differed most across children and adults after the full dosing regimen (V2). A total of eight features were selected following feature reduction by least absolute shrinkage and selection operator (LASSO). These eight features were used as input into a partial least-squares discriminant analysis (PLS-DA) to visualize the differences in vaccine-induced humoral immunity between children and adults (Figure 3A). Specifically, vaccine-induced S-specific ADNP, IgG4, FcγR2a, and ADCP were all enriched selectively in children, whereas Spike-specific FcαR binding antibodies, complement depositing antibodies, ADNKA (IFNγ secretion), and IgG2 titers were enriched in adults (**Figure 3B**). Importantly, in univariate profiling, children did not exhibit an inability to induce these responses at an overall population level, but some adults induced higher levels of these particular features (**Figure 2 and Supplemental Figure 2**). Conversely, multiple

features were enriched in children, pointing to enhanced functional immunity, rather than a deficit in the pediatric response to mRNA vaccination.

Because the feature reduction strategy aims to identify a minimal set of antibody features that differ most across the groups, additional features that co-correlate with the selected features may differ across the groups and provide enhanced mechanistic insights on biological differences in vaccine-induced immunity. Thus, we built a co-correlate network of additional features that were correlated with the markers that separated vaccinated children and vaccinated adults (**Figure 3C**). Three small clusters of co-correlates emerged highlighting additional features that were significantly ($p<0.05$, $|r|>0.7$) correlated with the LASSO-selected features that distinguished children and adults. The larger cluster was enriched in children, marking a relationship between Spike-specific ADNP and FcγR2a binding antibodies, highlighting the strong FcγR binding capacity and Fc mediated phagocytosis in children. Additional Spike-Fc-receptor binding levels were also linked to this cluster, highlighting the overall enhanced level of Fc-receptor binding responses induced following mRNA vaccination in children. The two additional clusters included features enriched in adults, marked by a cluster of S-specific NK cell activating antibodies that were all linked to one another and a network of IgA responses tied to FcαR binding. Additionally, vaccination induced higher titers and functions to SARS-CoV-2 than natural infection in children (**Figure 2 and Supplemental Figure 3**). Taken together, distinct humoral patterns were observed across adults and children immunized with the Moderna mRNA-1273 vaccine at the same dose, pointing to a bias towards a broad and robust Fc-receptor binding profile in children and a NK cell/IgA response in adults.

Real-world efficacy suggests that mRNA vaccines confer robust efficacy against severe disease/death against the original (wildtype; wt) SARS-CoV-2 strain (Wuhan), at levels greater than 90% (*19*). This level of efficacy appears to be sustained against the alpha and delta variants, although lower levels of protection have been observed against the beta variant(*20, 21*). Adaptive immunity and the ability to establish immune memory mature during the first decades of life. Several lines of evidence suggest that this more naïve immune response may adapt more easily to new antigens, able to generate broader and more flexible immunity to new viruses due to the robust production of naïve cells by the thymus and bone marrow in younger children (*22, 23*). Moreover, throughout life, our naïve clonal repertoire or immune cells shifts in response to the sequence of

pathogens and vaccines we are exposed to. Accordingly, more naïve children may have a less "biased" repertoire, enabling the generation of immunity to a broader range of pathogens(*24*). Thus, we next aimed to explore whether children generate vaccine responses against the variants of concern (VOCs)(*25*). As previously reported, we observed reduction in binding titer for all tested VOCs compared to the wildtype antigen for adult IgG1 responses (**Figure 4A**). Nearly identical binding patterns to VOCs were observed in children for IgG1 responses. While the patterns were very similar for additional IgG subclasses (IgG3) and isotypes (IgM), children induced slightly higher IgM responses to the VOCs than observed in adults. Furthermore, for most VOCs similar FcγR patterns were observed in children and adults, although slightly higher levels of FcγR binding was observed to the beta variant in children (**Figure 4B**). Virus neutralizing titers to the wildtype variant of SARS-CoV-2 were indistinguishable in children and adults, however a notable reduction in neutralizing activity was observed in children for the delta variant (**Figure 4C and Supplemental Figure 4**). Thus perhaps, using heterologous variant antigens for priming and boosting or pools of antigens, covering VOCs, could represent a strategy to broaden the pediatric immunity to current and future variants of SARS-CoV-2 or other coronaviruses(*26*). Importantly, despite this neutralization difference, wholistic comparison of the humoral immune response across the wildtype and the delta variant highlighted robust delta-neutralization and wildtype- and delta-ADNP and ADCP in children compared to adults (**Figure 4D and Supplemental Figure 4**). Moreover, following the second immunization, wildtype opsonophagocytic functions increased in children, marked by a vigorous delta-specific functional humoral immune response that may compensate for lower neutralization in this age group (**Figure 4E**). Additionally, vaccination resulted in more robust immunity to VOCs compared to natural infection in children (**Supplemental Figure 1 and 4**). Given our emerging appreciation for opsonophagocytic functions in protection against COVID-19 across natural infection, following vaccination in non-human primates, and following convalescent plasma, it is plausible that children may more robustly leverage this humoral mechanism, rather than neutralization alone, to maximized protection against disease(*12, 16, 17, 27*). Whether differences in neutralization and Fc-function lead to differences in disease-breakthrough across the ages remains unclear but provides some additional immunological insights that may continue to explain the epidemiologic differences in disease severity globally in the setting of emerging VOCs.

Collectively, children induced comparable neutralization but experienced a selective and preferential expansion of opsonophagocytic functions to both wildtype and VOCs compared to

adults via the selection of more robust Fc-receptor binding antibodies that may confer robust protection against infection and disease. This enhanced functionality was not linked to differential IgG subclass selection, or epitope targeting, suggesting that children may select distinct post-translational IgG modifications that may lead to more flexible, highly functional responses, that may represent an evolutionary adaptation enabling children to overcome infections in the setting of an evolving and maturing immune response. In adults, vaccination has consistently induced more robust immunity to SARS-CoV-2 than natural infection(*28*). Likewise, here we observed enhanced binding, neutralizing and Fc effector functions in vaccinated children compared to children diagnosed with COVID-19 or MIS-C, pointing to the importance of vaccination to robustly bolster immunity to SARS-CoV-2 and emerging variants of concern. However, larger cohorts, followed over time, will provide key insights into the precise protective titers, durability of mechanistic correlates of immunity in pediatric SARS-CoV-2 infection. Moreover, whether similar immunogenicity profiles will exist in even younger children, with a more naïve immune response, remains unclear, but points to the critical need to deeply profile the vaccine-induced immune response across ages, to gain novel insights into potential immune-vulnerabilities as well as unexpected immune strengths that may help explain differences in vaccine efficacy across the ages.

Materials and Methods

Cohort

Pediatric vaccinee samples were obtained from children who were vaccinated with two doses 100 μg mRNA-1273 at MGH as participants in Part 1 (open label) of a Phase2/3 clinical trial (ClinicalTrials.gov Identifier: NCT04796896). Additionally, we included samples from eight children who presented with acute PCR confirmed COVID-19 (7-19 years) or six children with MIS-C (3-22 years) at our hospital. Additionally, samples from 14 adults who received two doses mRNA-1273 as part of a phase 1 clinical trial were used as controls (ClinicalTrials.gov Identifier: NCT04283461). All pediatric participants provided informed assent and their legal guardian provided informed consent prior to participation in the observational MGH Pediatric COVID-19 Biorepository. Blood samples were collected prior to vaccination, one month after the first vaccination and one month after the second vaccination. This study was overseen and approved by the MassGeneral Institutional Review Board (IRB #2020P00955).

Antigens and biotinylation

All antigens were biotinylated using an NHS-Sulfo-LC-LC kit according to the manufacturer's instruction (Thermo Fisher, MA, USA) if required by the assay and excessive biotin was removed by size exclusion chromatography using Zeba-Spin desalting columns (7kDa cutoff, Thermo Fisher).

Antibody isotype and Fc receptor binding

Antigen-specific antibody isotype and subclass titers and Fc receptor binding profiles were analyzed with a custom multiplex Luminex assay as described previously (*29*). In brief, antigens were coupled directly to Luminex microspheres (Luminex Corp, TX, USA). Coupled beads were incubated with diluted plasma samples washed, and Ig isotypes or subclasses with a 1:100 diluted PE-conjugated secondary antibody for IgG1 (clone: HP6001), IgG2 (clone: 31-7-4), IgG3 (clone: HP6050), IgG4 (clone: HP6025), IgM (clone: SA-DA4), IgA1 (clone: B3506B4) or IgA2 (clone: A9604D2) (all Southern Biotech, AL, USA), respectively. For the FcγR binding, a respective PE–streptavidin (Agilent Technologies) coupled recombinant and biotinylated human FcγR protein was used as a secondary probe. Excessive secondary reagent was washed away after 1h incubation, and the relative antigen-specific antibody levels were determined on an iQue analyzer (Intellicyt).

Antibody-Dependent Complement Deposition (ADCD)

Complement deposition was performed as described before(*30*). In brief, biotinylated antigens were coupled to FluoSphere NeutrAvidin beads (Thermo Fisher) and to form immune-complexes incubated with 10 μl 1:10 diluted plasma samples for 2h at 37°C. After non-specific antibodies were washed away, immune-complexes were incubated with guinea pig complement in GVB++ buffer (Boston BioProducts, MA, USA) for 20 min at 37°C. EDTA containing PBS (15mM) was used to stop the complement reaction and deposited C3 on beads was stained with anti-guinea pig C3-FITC antibody (MP Biomedicals, CA, USA, 1:100, polyclonal) and analyzed on an iQue analyzer (Intellicyt).

Antibody-Dependent-Neutrophil-Phagocytosis (ADNP)

Phagocytosis score of primary human neutrophils was determined as described before(*31*). Biotinylated antigens were coupled to FluoSphere NeutrAvidin beads (Thermo Fisher) and incubated with 10 μl 1:100 diluted plasma for 2h at 37°C to form immune-complexes. Primary neutrophils were derived from Ammonium-Chloride-Potassium (ACK) buffer lysed whole blood from healthy donors and incubated with washed immune complexes for 1h at 37°C. Afterwards, neutrophils were stained for surface CD66b (Biolegend, CA, USA; 1:100, clone: G10F5) expression, fixed with 4% para-formaldehyde and analyzed on a iQue analyzer (Intellicyt).

Antibody-Dependent-THP-1 Cell-Phagocytosis (ADCP)

THP-1 phagocytosis assay was performed as described before(*32*). In brief, biotinylated antigens were coupled to FluoSphere NeutrAvidin beads (Thermo Fisher) and incubated with 10 µl 1:100 diluted plasma for 2h at 37°C to form immune complexes. THP-1 monocytes were added to the beads, incubated for 16 h at 37°C, fixed with 4% para-formaldehyde and analyzed on a iQue analyzer (Intellicyt).

Antibody-Dependent-NK-Activation (ADNKA)

To determine Antibody-dependent NK cell activation, MaxiSporp ELISA plates (Thermo Fisher) were coated with respective antigen for 2h at RT and then blocked with 5% BSA (Sigma-Aldrich). 50 µl 1:50 diluted plasma sample or monoclonal Abs was added to the wells and incubated overnight at 4°C. NK cells were isolated from buffy coats from healthy donors using the RosetteSep NK cell enrichment kit (STEMCELL Technologies, MA, USA) and stimulated with rhIL-15 (1ng/ml, STEMCELL Technologies) at 37°C overnight. NK cells were added to the washed ELISA plate and incubated together with anti-human CD107a (BD, 1:40, clone: H4A3), brefeldin A (Sigma-Aldrich, MO, USA), and monensin (BD) for 5 hours at 37°C. Next, cells were surface stained for CD56 (BD, 1:200, clone: B159), CD16 (BD, 1:200, clone: 3G8), and CD3 (BD, 1:800, UCHT1). After fixation and permeabilization with FIX & PERM Cell Permeabilization Kit (Thermo Fisher), cells were stained for intracellular markers MIP1β (BD, 1:50, clone: D21-1351) and IFNγ (BD, 1:17, clone: B27). NK cells were defined as CD3-CD16+CD56+ and frequencies of degranulated (CD107a+), INFγ+ and MIP1β+ NK cells determined on an iQue analyzer (Intellicyt)(*33*).

Virus neutralization

Three-fold serial dilutions ranging from 1:12 to 1:8748 were performed for each plasma sample before adding 50–250 infectious units of pseudovirus expressing the SARS-CoV-2 reference (Wuhan/wildtype) or delta variant Spike to hACE-2 expressing HEK293 cells for 1 hour. Percentage neutralization was determined by subtracting background luminescence measured in cell control wells (cells only) from sample wells and dividing by virus control wells (virus and cells only). Pseudovirus neutralization titers (pNT50) values were calculated by taking the inverse of the 50% inhibitory concentration value for all samples with a pseudovirus neutralization value of 80% or higher at the highest concentration of serum.

Data analysis and Statistics

Data analysis was performed using GraphPad Prism (v.9.2.0) and RStudio (v.1.3 and R v.4.0). Comparisons between the adults and children were performed using Wilcoxon-signed rank test followed by Benjamini-Hochberg (BH) correction. Heatmap was generated using the pheatmap package (v.1.0.12) in R using Z-scored values. Multivariate classification models were built to discriminate humoral profiles between vaccination arms. Prior to analysis, all data were normalized using z-scoring. Feature selection was performed using least absolute shrinkage and selection operator (LASSO). Classification and visualization were performed using partial least square discriminant analysis (PLS-DA). Model accuracy was assessed using ten-fold cross-validation. These analyses were performed using R package "ropls" version 1.20.0 (*34*) and "glmnet" version 4.0.2(*35*). Co-correlates of LASSO selected features were calculated to find features that can equally contribute to discriminating vaccination arms. Correlations were performed using Spearman method followed by Benjamini-Hochberg correction. The co-correlate network was generated using R package "network" version 1.16.0(*36*). Flower plots were generated using the ggplot (v.3.3.5) package in R. Values were Z-scored per feature and antigen but using the data for all timepoints.

References and Notes

1. L. R. Baden *et al.*, Efficacy and Safety of the mRNA-1273 SARS-CoV-2 Vaccine. *N Engl J Med* **384**, 403-416 (2021).
2. F. P. Polack *et al.*, Safety and Efficacy of the BNT162b2 mRNA Covid-19 Vaccine. *N Engl J Med* **383**, 2603-2615 (2020).
3. V. T. Chu *et al.*, Household Transmission of SARS-CoV-2 from Children and Adolescents. *N Engl J Med* **385**, 954-956 (2021).
4. L. M. Yonker *et al.*, Pediatric Severe Acute Respiratory Syndrome Coronavirus 2 (SARS-CoV-2): Clinical Presentation, Infectivity, and Immune Responses. *J Pediatr* **227**, 45-52 e45 (2020).
5. L. M. Yonker *et al.*, Virologic features of SARS-CoV-2 infection in children. *medRxiv*, (2021).
6. J. F. Ludvigsson, Systematic review of COVID-19 in children shows milder cases and a better prognosis than adults. *Acta Paediatr* **109**, 1088-1095 (2020).
7. M. J. Delahoy *et al.*, Hospitalizations Associated with COVID-19 Among Children and Adolescents - COVID-NET, 14 States, March 1, 2020-August 14, 2021. *MMWR Morb Mortal Wkly Rep* **70**, 1255-1260 (2021).
8. D. A. Siegel *et al.*, Trends in COVID-19 Cases, Emergency Department Visits, and Hospital Admissions Among Children and Adolescents Aged 0-17 Years - United States, August 2020-August 2021. *MMWR Morb Mortal Wkly Rep* **70**, 1249-1254 (2021).
9. J. Bonhoeffer, C. A. Siegrist, P. T. Heath, Immunisation of premature infants. *Arch Dis Child* **91**, 929-935 (2006).
10. S. P. Weisberg *et al.*, Distinct antibody responses to SARS-CoV-2 in children and adults across the COVID-19 clinical spectrum. *Nat Immunol* **22**, 25-31 (2021).
11. E. R. Stiehm, H. H. Fudenberg, Serum levels of immune globulins in health and disease: a survey. *Pediatrics* **37**, 715-727 (1966).
12. T. Zohar *et al.*, Compromised Humoral Functional Evolution Tracks with SARS-CoV-2 Mortality. *Cell* **183**, 1508-1519 e1512 (2020).
13. C. E. Z. Chan *et al.*, The Fc-mediated effector functions of a potent SARS-CoV-2 neutralizing antibody, SC31, isolated from an early convalescent COVID-19 patient, are essential for the optimal therapeutic efficacy of the antibody. *PLoS One* **16**, e0253487 (2021).
14. M. J. Gorman *et al.*, Fab and Fc contribute to maximal protection against SARS-CoV-2 following NVX-CoV2373 subunit vaccine with Matrix-M vaccination. *Cell Rep Med*, 100405 (2021).
15. J. M. Woof, M. A. Kerr, IgA function--variations on a theme. *Immunology* **113**, 175-177 (2004).
16. K. McMahan *et al.*, Correlates of protection against SARS-CoV-2 in rhesus macaques. *Nature* **590**, 630-634 (2021).
17. J. R. Francica *et al.*, Protective antibodies elicited by SARS-CoV-2 spike protein vaccination are boosted in the lung after challenge in nonhuman primates. *Sci Transl Med* **13**, (2021).
18. S. Chakraborty *et al.*, Proinflammatory IgG Fc structures in patients with severe COVID-19. *Nat Immunol* **22**, 67-73 (2021).
19. E. J. Haas *et al.*, Impact and effectiveness of mRNA BNT162b2 vaccine against SARS-CoV-2 infections and COVID-19 cases, hospitalisations, and deaths following a

nationwide vaccination campaign in Israel: an observational study using national surveillance data. *Lancet* **397**, 1819-1829 (2021).

20. J. S. Tregoning, K. E. Flight, S. L. Higham, Z. Wang, B. F. Pierce, Progress of the COVID-19 vaccine effort: viruses, vaccines and variants versus efficacy, effectiveness and escape. *Nat Rev Immunol* **21**, 626-636 (2021).
21. L. J. Abu-Raddad, H. Chemaitelly, A. A. Butt, C.-V. National Study Group for, Effectiveness of the BNT162b2 Covid-19 Vaccine against the B.1.1.7 and B.1.351 Variants. *N Engl J Med* **385**, 187-189 (2021).
22. A. Vatti *et al.*, Original antigenic sin: A comprehensive review. *J Autoimmun* **83**, 12-21 (2017).
23. J. J. Goronzy, C. M. Weyand, T cell development and receptor diversity during aging. *Curr Opin Immunol* **17**, 468-475 (2005).
24. L. Garderet *et al.*, The umbilical cord blood alphabeta T-cell repertoire: characteristics of a polyclonal and naive but completely formed repertoire. *Blood* **91**, 340-346 (1998).
25. P. Kaplonek *et al.*, Subtle immunological differences in mRNA-1273 and BNT162b2 COVID-19 vaccine induced Fc-functional profiles. *bioRxiv*, (2021).
26. A. Choi *et al.*, Safety and immunogenicity of SARS-CoV-2 variant mRNA vaccine boosters in healthy adults: an interim analysis. *Nat Med*, (2021).
27. H. Natarajan *et al.*, Markers of Polyfunctional SARS-CoV-2 Antibodies in Convalescent Plasma. *mBio* **12**, (2021).
28. L. A. Jackson *et al.*, An mRNA Vaccine against SARS-CoV-2 - Preliminary Report. *N Engl J Med* **383**, 1920-1931 (2020).
29. E. P. Brown *et al.*, High-throughput, multiplexed IgG subclassing of antigen-specific antibodies from clinical samples. *J Immunol Methods* **386**, 117-123 (2012).
30. S. Fischinger *et al.*, A high-throughput, bead-based, antigen-specific assay to assess the ability of antibodies to induce complement activation. *J Immunol Methods* **473**, 112630 (2019).
31. C. B. Karsten *et al.*, A versatile high-throughput assay to characterize antibody-mediated neutrophil phagocytosis. *J Immunol Methods* **471**, 46-56 (2019).
32. M. E. Ackerman *et al.*, A robust, high-throughput assay to determine the phagocytic activity of clinical antibody samples. *Journal of immunological methods* **366**, 8-19 (2011).
33. L. L. Lu *et al.*, A Functional Role for Antibodies in Tuberculosis. *Cell* **167**, 433-443 e414 (2016).
34. E. A. Thevenot, A. Roux, Y. Xu, E. Ezan, C. Junot, Analysis of the Human Adult Urinary Metabolome Variations with Age, Body Mass Index, and Gender by Implementing a Comprehensive Workflow for Univariate and OPLS Statistical Analyses. *J Proteome Res* **14**, 3322-3335 (2015).
35. J. H. Friedman, T. Hastie, R. Tibshirani, Regularization Paths for Generalized Linear Models via Coordinate Descent. *2010* **33**, 22 (2010).
36. C. T. Butts, network: a Package for Managing Relational Data in R. *Journal of Statistical Software* **24**, (2008).

Acknowledgments: We would like to thank Caroline Atyeo for her support. We thank Nancy Zimmerman, Mark and Lisa Schwartz, an anonymous donor (financial support), Terry and Susan Ragon, and the SAMANA Kay MGH Research Scholars award for their support. We acknowledge support from the Ragon Institute of MGH, MIT, and Harvard, the Massachusetts Consortium on Pathogen Readiness (MassCPR) and the Musk foundation. This work used samples from the phase 1 mRNA-1273 study (NCT04283461; DOI: 10.1056/NEJMoa2022483). The mRNA-1273 phase 1 study was sponsored and primarily funded by the National Institute of Allergy and Infectious Diseases (NIAID), National Institutes of Health (NIH), Bethesda, MD. This trial has been funded in part with federal funds from the NIAID under grant awards UM1AI148373, to Kaiser Washington; UM1AI148576, UM1AI148684, and NIH P51 OD011132, to Emory University; NIH AID AI149644, and contract award HHSN272201500002C, to Emmes. Funding for the manufacture of mRNA-1273 phase 1 material was provided by the Coalition for Epidemic Preparedness Innovation.

Funding:

NIH 3R37AI080289-11S1,

NIH R01AI146785,

NIH U19AI42790-01,

NIH U19AI135995-02,

NIH U19AI42790-01,

NIH 1U01CA260476 – 01,

NIH CIVIC75N93019C00052

The Gates Foundation Global Health Vaccine Accelerator Platform funding OPP1146996

The Gates Foundation Global Health Vaccine Accelerator Platform funding INV-001650

Author contributions: Y.C.B. and J.K. performed the serological experiments. K.S.D, E.C.L. and A.B.B. performed the neutralization assay. Y.C.B., L.M.Y. and G.A. analyzed and interpreted the data. E.J.F., J.D., B.B., W.S. and L.M.Y. supervised and managed the clinical trial. G.A. supervised the project. Y.C.B., L.M.Y. and G.A. drafted the manuscript. All authors critically reviewed the manuscript.

Competing interests: G.A. is a founder and equity holder of Seromyx Systems, a company developing a platform technology that describes the antibody immune response. G.A. is an employee and equity holder of Leyden Labs, a company developing pandemic prevention therapeutics. G.A.'s interests were reviewed and are managed by Massachusetts General Hospital and Partners HealthCare in accordance with their conflict of interest policies. All other authors have declared that no conflicts of interest exist.

Data and materials availability: All data are available in the main text or the supplementary materials.

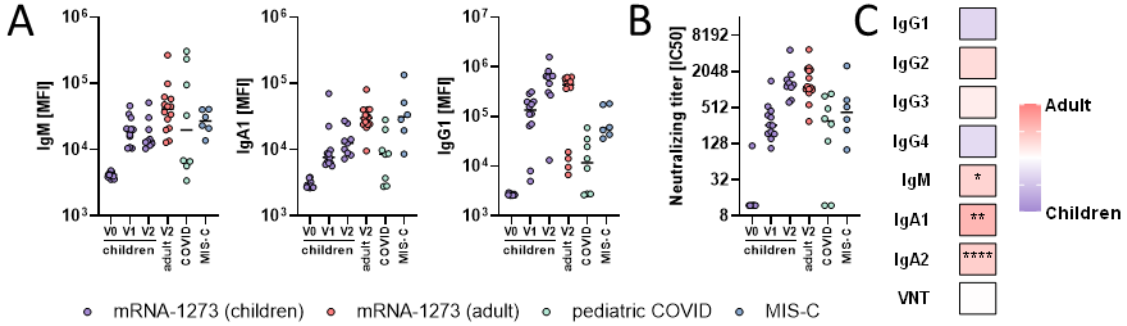

Figure 1. mRNA-1273 vaccination induces robust binding and neutralizing titers in children. Binding and neutralizing titers were analyzed in children (7-11 years) before (V0, n=12), after the first (V1, n=12) or after the second (V2, n=9) dose or adults after the second dose (V2, n=14) of the mRNA-1273 vaccine as well as during acute pediatric COVID (n=8) or MIS-C (n=6). A) Relative SARS-CoV-2 Spike (Wuhan) specific IgM, IgA1 and IgG1 binding levels were determined by Luminex. B) The dot plots show virus neutralizing titers, at which 50 % reduction of infection of a SARS-CoV-2 Spike pseudovirus was observed. C) Tiles indicate whether antibody binding features were upregulated in fully vaccinated children (blue shades) or adults (red shades) at V2. A Wilcoxon-rank test was used to test for statistical significance and asterisks indicate statistically significant differences after Benjamini-Hochberg correction for multiple testing (*:$p<0.05$; **:$p<0.01$;***:$p<0.001$).

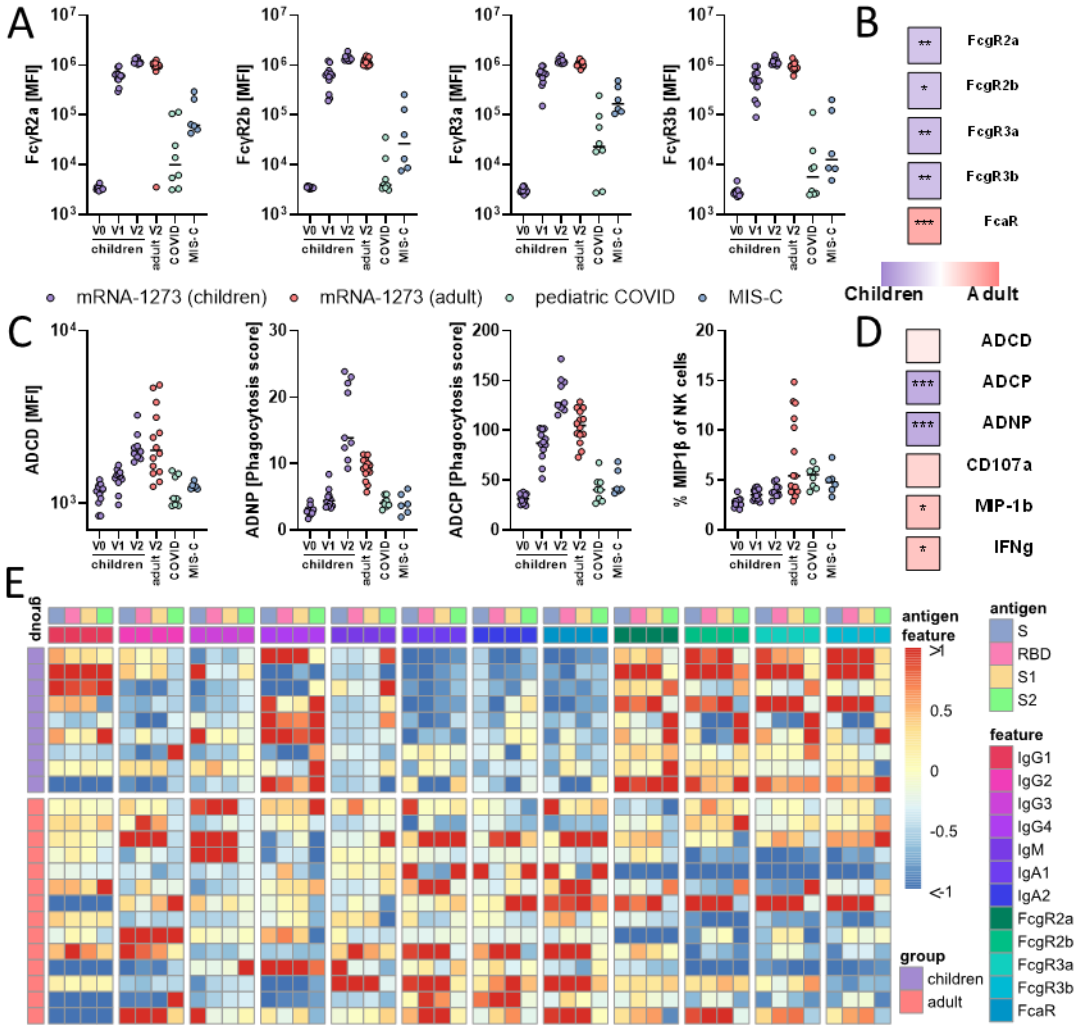

Figure 2. mRNA-1273 vaccination induces higher FcγR binding and phagocytic activity in children. A) Binding of SARS-CoV-2 specific antibodies to FcγR2a, 2b, 3a, and 3b was determined by Luminex in children (7-11 years) before (V0, n=12), after the first (V1, n=12) or after the second (V2, n=9) dose or adults after the second dose (V2, n=14) of the mRNA-1273 vaccine as well as during acute pediatric COVID (n=8) or MIS-C (n=6). B) Tiles indicate whether FcγR binding features were upregulated in fully vaccinated children (blue shades) or adults (red shades) at V2. C) The ability of SARS-CoV-2 S specific antibody Fc to induce antibody-dependent-complement-deposition (ADCD), neutrophil-phagocytosis (ADNP), cellular-THP1 monocyte-phagocytosis (ADCP), or activation of NK cells marked by expression of MIP-1β was analyzed. D) Tiles indicate whether Fc functions were upregulated in fully vaccinated children (blue shades) or adults (red shades) at V2. A Wilcoxon-rank test was used to test for statistical significance in B) and D) and asterisks indicate statistically significant differences after Benjamini-Hochberg correction for multiple testing (*:p<0.05; **:p<0.01;***:p<0.001). E) The heatmap shows the Z-scored antibody titers or Fcγ receptor binding levels (as indicated by the feature color key for values from -1 to 1, values above or below this limit were assigned maximum values (1) or minimal (-1) values) for SARS-CoV-2 full Spike, receptor binding domain (RBD), S1 and S2 domain responses (as indicated by the antigen color key) in fully vaccinated children or adults (purple or red, respectively, as indicated by the group color key).

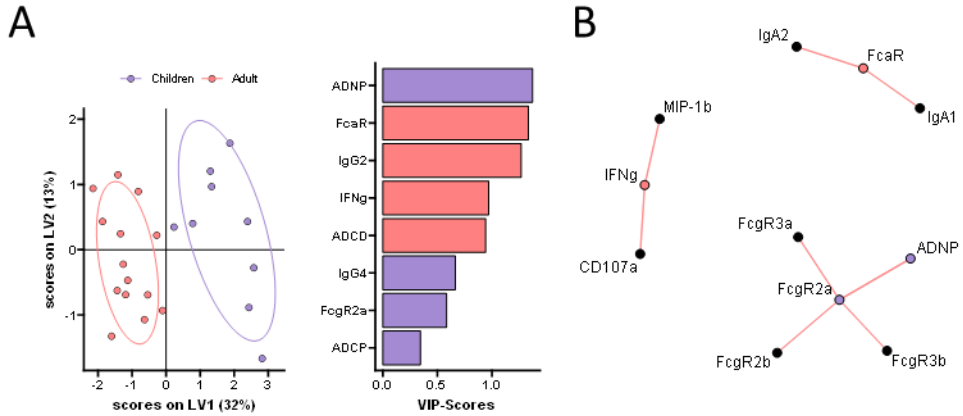

Figure 3. Distinct humoral profiles distinguish between adult and pediatric vaccine responses. A) A machine learning model was built using a minimal set of LASSO selected SARS-CoV-2 S specific features at V2 (left panel) to discriminate between vaccine responses in adult (red, n=14) and children (purple, n=9) in a PLS-DA analysis (right panel). B) The co-correlation network illustrates all LASSO-selected features. Nodes of selected features are colored whether they were enriched in children (purple) or adults (red). Lines indicate significant ($p<0.05$) spearman correlations with $|r|>0.7$ of connected features (only positive correlations with $r>0$ were observed).

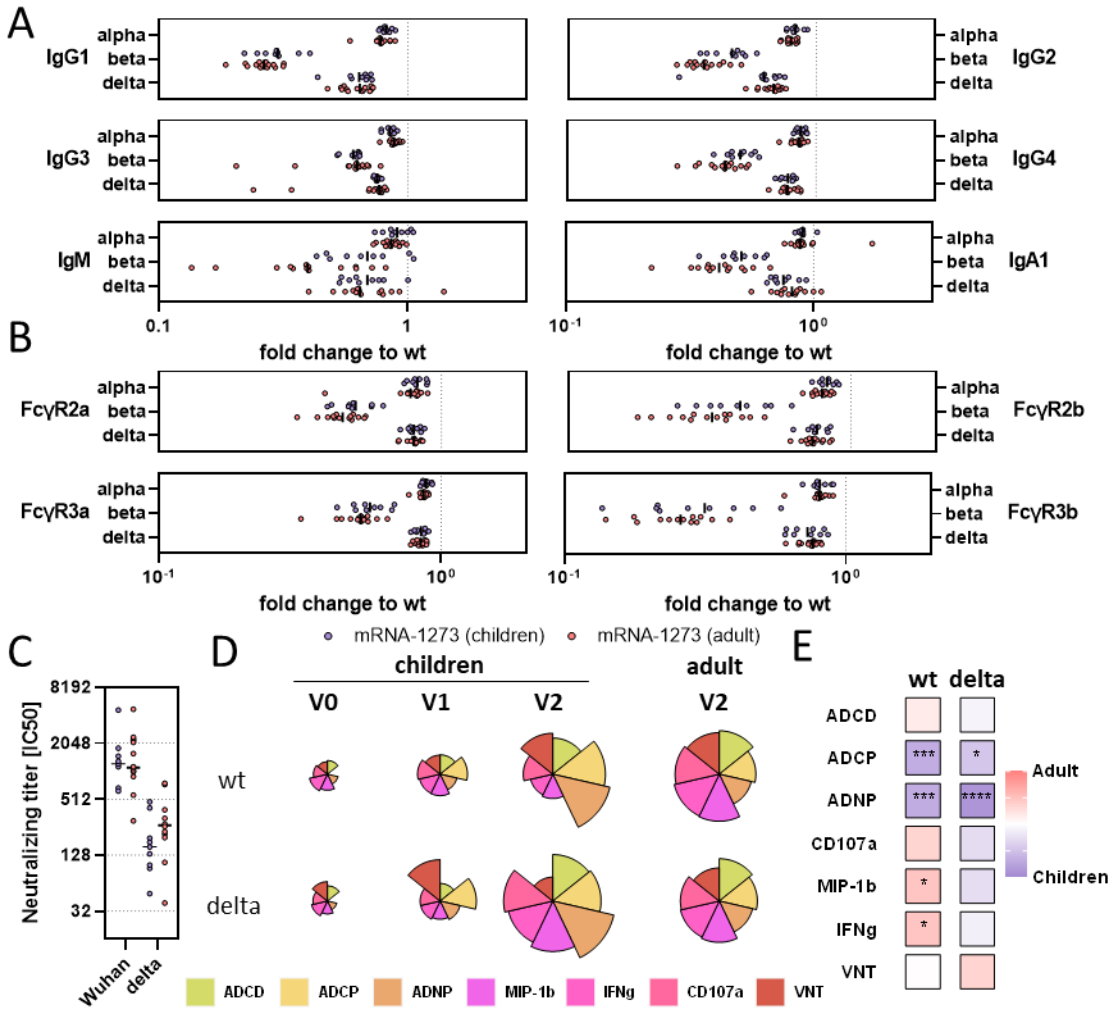

Figure 4. mRNA-1273 vaccination elicits humoral responses to SARS-CoV-2 variants of concern. A) Vaccine induced subclass and isotype RBD-specific titers are shown for children or adults at V2 relative to the WT RBD. B) FcγR binding profiles of vaccine induced RBD specific antibodies in children (n=9) or adults (n=14) at V2 relative to the WT RBD. C) Virus neutralizing titers are shown to the wildtype (wt) or the delta variant in children or adults at V2. D) The flower plots summarize functional antibody responses to the SARS-CoV-2 wt (Wuhan; top) or delta (bottom) variant specific S in children at V0, V1 and V2 or adults at V2. The color of each petal corresponds to the respective feature and the length of the petal to the average after the data was Z-scored. E) Tiles indicate whether Fc functions were upregulated in fully vaccinated children (blue shades) or adults (red shades) at V2 for wt or delta variant (compare Figure 2). A Wilcoxon-rank test was used to test for statistical significance A), B) and E) and asterisks indicate statistically significant differences after Benjamini-Hochberg correction for multiple testing (*:p<0.05; **:p<0.01;***:p<0.001).